Predictions of Fluid/Structural Interactions Using Abaqus Cosimulation and Advanced CFD Solvers

Peter A. Cavallo

Combustion Research and Flow Technology, Inc. (CRAFT Tech)

***Abstract**: This work presents a coupled fluid-structural interaction (FSI) capability wherein pressure and thermal loads predicted by the CRUNCH CFD® and CRAFT CFD® Navier-Stokes solvers are exchanged with Abaqus/Standard and Abaqus/Explicit using the Co-Simulation Engine (CSE). Multiple domains may be simulated concurrently, on separate groups of processors. Data exchange is handled through SIMULIA's Co-Simulation Engine API. The boundary surface common to the fluid and solid domains is defined, along with the specific scalar and/or vector fields to be exchanged. Point forces or pressures, heat fluxes, displacements, and temperatures are passed between the codes, and simulations may be either one-way or two-way coupled. Applications of the FSI simulation capability to problems of interest are presented and discussed.*

***Keywords**: CFD Coupling, Coupled Analysis, Design Optimization, Heat Transfer, Plasticity, Vibration.*

1. Introduction

Multidisciplinary analysis and optimization are increasingly areas of interest for the design of practical engineering systems. Constraints on size, weight, and performance specifications require the analyst to examine how a solution for one aspect of the system affects others to achieve an ideal design. Traditionally, different groups within an organization have addressed their portion of the overall analysis, relying upon the results of other groups for inputs on loads, boundary conditions, *etc*. Such loosely coupled analysis can neglect potential first order effects of one aspect of the design on another, and impact both development schedule and cost.

To address this issue, computer-aided engineering simulation has been driven to incorporate various disciplines under one roof. The evolution of "multi-physics" software has allowed engineers to assess the impact of specific design decisions on the overall product earlier in the design cycle. Simulation codes developed to analyze solid mechanics, fluid flow, noise generation, heat transfer, *etc*. may be combined to provide unparalleled insight into product performance. Towards that end, SIMULIA has developed a Co-Simulation Engine (CSE) and Application Programming Interface (API) to facilitate the integration of 3rd party codes with Abaqus/Standard and Abaqus/Explicit.

This paper presents an overview of CRAFT Tech's efforts in coupling Abaqus with its CFD solvers for simulating fluid-structural interaction (FSI) problems with advanced flow physics. A summary of the coupling methodology and interfacing with the CSE is provided. Applications of the FSI simulation capability are described, which include the use of Abaqus in vibration, heat transfer, plastic deformation, and design optimization studies. Potential future directions for development and analysis are offered in concluding remarks.

2. CFD Codes and Code Coupling

This section provides a synopsis of how Abaqus was coupled with CRAFT Tech's Navier-Stokes solvers, *CRUNCH CFD*® (Hosangadi, 1998) and *CRAFT CFD*® (Kannepalli, 2011). Pre-processing tools were also developed to facilitate analysis. Specific utilities include grid conversion to embed meshes produced by the 3rd party software Pointwise (Pointwise) into the Abaqus input file, and automated setup of the Abaqus input with material properties, boundary conditions, cosimulation interface, and constraints defined.

2.1 Navier-Stokes Solvers

Most fluid simulations conducted by CRAFT Tech employ the unstructured grid *CRUNCH CFD*® code (Hosangadi, 1998). *CRUNCH CFD*® uses a second order finite volume upwind Roe scheme in which the flow variables are defined at the vertices of the mesh. The solver supports mixed-element grids containing tetrahedra, pyramids, prisms, and hexahedral cell types. Turbulence modeling is provided by the Spalart-Allmaras, k-ε, or k-ω models, with compressibility and near-wall modeling extensions available for certain classes of flows. As a general purpose solver, models are also available for combustion, cavitation, particulates, *etc*.

For cases requiring high spatial fidelity, the structured grid *CRAFT CFD*® code (Kannepalli, 2011) is used. For steady Reynolds-Averaged (RANS) computations, a 3rd order upwind biased scheme is employed, while for transient LES calculations, a 5th order scheme is available. This is a high order accurate scheme which has been extensively validated for aeroacoustics. Turbulence modeling is provided by a k-ε model, with various extensions for near wall and compressibility treatments.

CRAFT Tech's multi-physics framework greatly facilitated the integration of Abaqus. The multi-physics framework is comprised of various modules that may be run concurrently, including *CRUNCH CFD*®, *CRAFT CFD*®, a heat conduction solver, a noise propagation code, and now a structural module to invoke Abaqus. Multiple modules are launched on separate groups of processors, to simulate advanced applications. Examples include rotor-stator problems, conjugate heat transfer, and now, fluid-structural interaction. In applications to date, Abaqus runs in the background, a single processor handles the data exchange with both the CSE and the fluid domains that are to communicate with Abaqus, while many parallel processors solve the fluid domain. The groups of processors are synchronized at each time step to advance the fluid and the solid domains.

2.2 Integration of Cosimulation Engine (CSE)

Data exchange between *CRUNCH CFD*® or *CRAFT CFD*® and Abaqus is handled through SIMULIA's Co-Simulation Engine API. Using API library calls, the boundary surface common to the fluid and solid domains is defined, along with the specific scalar and/or vector fields to be exchanged. Currently, point forces and displacements are passed between the codes, though in general other fields such as temperatures may be used. In addition, the API is used to define the target time step. If necessary, Abaqus may take several substeps to advance its solution to match the time step taken by the fluid. Table 1 lists the relevant calls to the CSE that are made by the processor handling the Abaqus exchanges.

Table 1. CSE API Calls.

Establish connection to Abaqus	SMACseInitialize( ); strcpy(cseDirectorString,hostport); SMACseConnect(codeName,jobName,workDir,cseDirectorString,timeout, startTime,PutField,userData,ErrorHandler);

Define FSI boundary face and vertex definitions	SMACseMesh* mesh = SMACseCreateMesh("FSI Nodes");
	SMACseAddNodeCollection(mesh,"Node Collection",
	SMACseDim_3d,num_nodes,labels,coords);
	if(num_quads > 0) {
	for (i=0; i<num_quads; i++) {
	qlabels[i] = i+1;
	}
	SMACseAddElemCollection(mesh,"Quads","Node Collection",
	"SMACseSurfTopo_Quad4",num_quads,qlabels,nquad_conn);
	}
	SMACseRegisterMesh(mesh);

Define fields to be imported and exported by Abaqus – must match the XML configuration file	SMACseCreateFieldDefinition("displacement",SMACseFieldPos_atNode, SMACseFieldAlgType_Vector3d,SMACseFieldDataType_Double); SMACseCreateFieldDefinition("force",SMACseFieldPos_atNode, SMACseFieldAlgType_Vector3d,SMACseFieldDataType_Double); SMACseRegisterIncomingField("displacement","FSI Nodes", SMACseUnitSystem_Consistent); SMACseRegisterOutgoingField("force","FSI Nodes", SMACseUnitSystem_Consistent);

Specify the Abaqus time step	status = SMACseGetTargetTime(currtime,currstep,&targetTime,&currstep,&lockstep);
	status = SMACseNotifyStart( );
	SMACseGetField("displacement",nnodes,labels,targetTime,disp,nnodes*sizeof(double),NULL);
	status = SMACseNotifyEnd(targetTime);

Break the connection to Abaqus	SMACseDisconnect( ); SMACseFinalize( );

In addition, the Abaqus input must include commands dictating which fields are passed between codes. This information is also included in a configuration XML file, which completes the setup.

```
*CO-SIMULATION, NAME=CRUNCHCFD, PROGRAM=MULTIPHYSICS
*CO-SIMULATION REGION, IMPORT
INTERFACE, CF
INTERFACE, HFL
*CO-SIMULATION REGION, EXPORT
INTERFACE, U
INTERFACE, NT
```

The multi-physics framework implements a master controller, shown in Figure 1, which perform an MPI_COMM_SPLIT for each module to be invoked. The module that treats data transfer to Abaqus and makes calls to the CSE API, known as the CSE Interface Process, uses a single processor, as Abaqus is launched in the background prior to execution. Additional modules may use any number of processors to compute one or more fluid domains as shown.

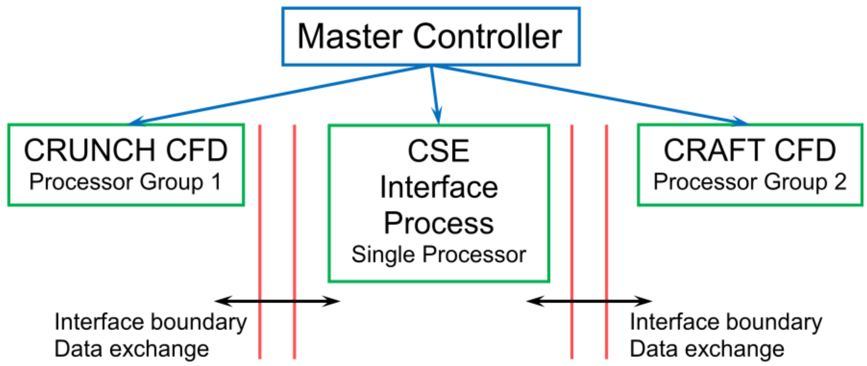

Figure 1. Schematic of CRAFT Tech multi-physics framework.

In a one-way coupled analysis, where displacements are assumed to have a negligible impact on the flow field, the CFD simulation need not be run in tandem with the structural analysis. Rather, the transient pressure or thermal loads may be saved to a series of data files and "replayed" for analysis by Abaqus. This permits the same load to be applied to a variety of designs, constraints, and configurations, for the purpose of parametric design analysis or design optimization. Pressure and/or heat transfer data is then provided at suitable time intervals that can capture the structural frequency response. For such applications, the CSE Interface Process still handles the data exchange to Abaqus and also handles the saved data file I/O.

2.3 Mesh Movement

For FSI applications where the predicted deflections are small, a one-way coupled approach may be sufficient. Forces from the fluid domain are passed to the solid domain, and the structure undergoes deformation. However these deformations are ignored by the fluid domain and the fluid boundaries do not change. In cases where the predicted deflections are substantial, a two-way coupling has been established and demonstrated. The additional complexity involves the application of the surface deflections predicted by Abaqus to the fluid grid. A mesh movement solver must be employed to redistribute the nodes in the fluid domain. Two mesh movement schemes are available in *CRUNCH CFD*® to accomplish this task (Allen, 2006, Cavallo, 2005). Since moving the grid incurs additional computational cost, two-way coupled analyses are inherently more expensive. In applications to date, an algebraic mesh movement solver (Allen, 2006) is employed to help minimize this cost.

3. Applications

3.1 Jet Blast Deflector

The integration of current and future aircraft with ship operations is of continuing interest to the US Navy. Manned and unmanned aircraft under development must be cleared to perform takeoff and landing scenarios. Figure 2 depicts a naval jet blast deflector, which is comprised of multiple panels that may be individually raised and lowered. Each panel consists of a plate supported by two struts at the rear, with a series of cooling channels that serve to remove the heat of the jet blast. Nominal cooling passages were assumed in which water at 60°F flows at a rate of 100 gal/min. For the sake of this exploratory demonstration, the JBD plates are angled at 50° relative to horizontal, assumed to be constant thickness, and the cooling passages are placed adjacent to the structure.

Figure 2. Jet blast deflector being serviced aboard a Navy ship.

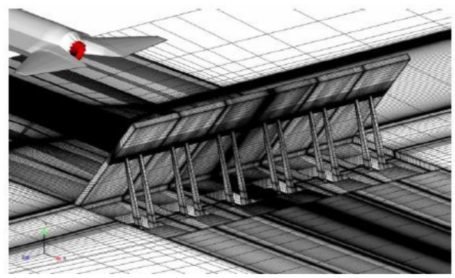

Figure 3. CFD mesh of jet and surrounding JBD regions.

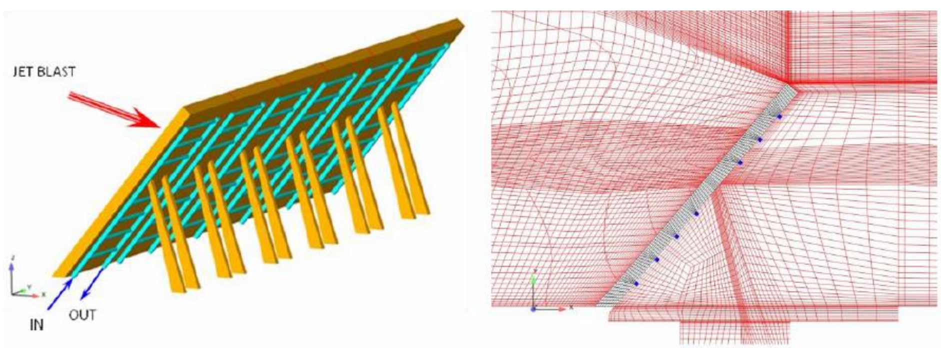

(a) Problem overview (b) Meshes for three simulation modules

Figure 4. Assumed coolant passages and their placement.

Figure 3 illustrates the structured grid employed in the jet simulation. Figure 4 depicts the simplified cooling channel geometry and a slice through the volume grid highlighting each of the three domains in the coupled FSI simulation. The red mesh denotes the jet flowfield, simulated with *CRAFT CFD*®, the black mesh represents the JBD itself, computed with Abaqus, and the blue mesh is the incompressible coolant flow, simulated with *CRUNCH CFD*®. Each of the cooling channels is separate, with a unique inlet and outlet for the water flow, and the exit pressure is allowed to float to match the prescribed volumetric flow rate.

The simulations are initiated from a steady state isothermal simulation in which an assumed constant wall temperature is applied for all of the JBD surfaces. During the coupled FSI simulation, the local heat flux is modified to reflect the current local temperature distribution as predicted by Abaqus. For stability, Abaqus is invoked once every 100 CFD iterations to allow the adjacent fluid domains to adjust to each change in the wall temperatures. Coupled iterations proceed until the net heat flux into and out of the solid domain is nearly zero, wherein the solution is considered to be converged. This heat flux is monitored by the CSE Interface Process.

A key item of interest is the resulting stresses induced in the structure from the pressure and thermal loadings. Figure 6 shows the stress distribution in the JBD as viewed from the front and from the rear. The structure is constrained at the base of each plate, as well as at the base of each of 12 struts supporting the JBD. Peak stresses are noted to be at the plate base as well as where the JBD plates meet the support struts, as expected.

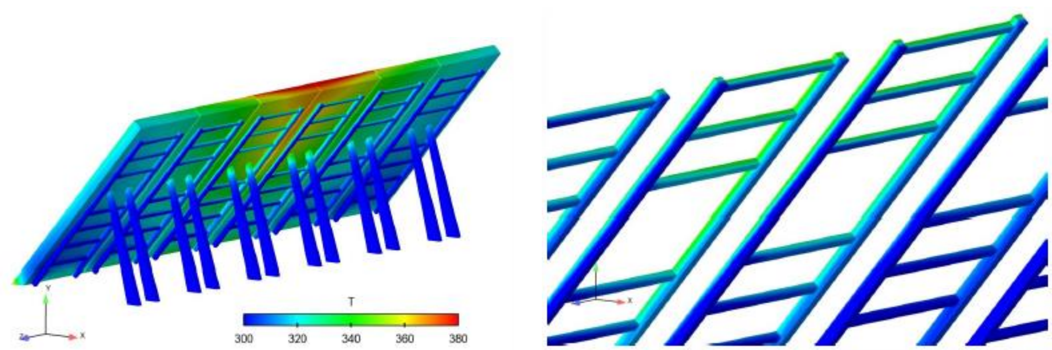

(a) Rear view of JBD and coolant flow (b) Close-up of center coolant passages

Figure 5. Temperature distribution in coolant passages.

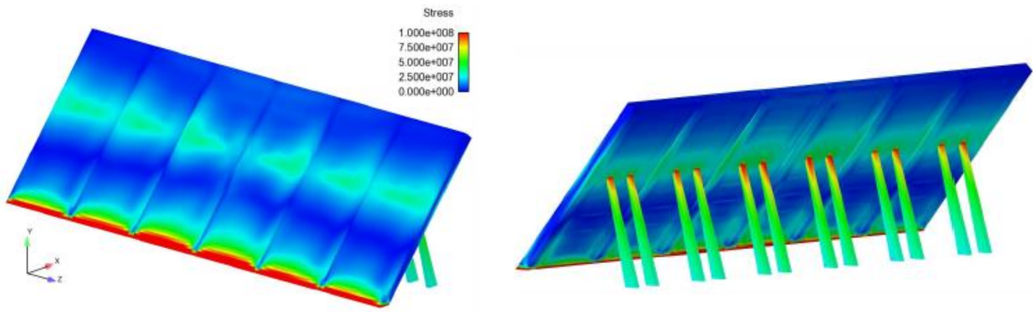

(a) Front View (b) Rear View

Figure 6. Stresses in the JDB plates and supports.

3.2 Rupture of a Pressurized Canister

The next demonstration considers plastic deformation of a metal canister containing water which ruptures. The release of the bulk liquid and droplets is simulated with *CRAFT CFD*® using Eulerian droplet tracking and localized breakup and vaporization models. An initial crack is assumed and built into the model, along with an assumed hole. Within Abaqus/Explicit, the `*PLASTIC` option was enabled and a yield stress specified.

Figure 7 presents the evolution of the plastic deformation produced by the shock reflections inside the canister and the resulting expulsion of the water, as viewed from above. The initial crack created in the model expands dramatically, and at 2 msec of elapsed time the hole is substantial. Contours of the resulting Von Mises stress are depicted in Figure 8. Here the contours are clipped at the yield stress of the steel, so that stresses producing plastic deformation are clearly visible in red. The initial time points highlight the stress propagating through the material from the point where the crack opens. The bulk liquid and droplet flyout at selected instants in time is illustrated in Figure 9. The fine small diameter droplets are depicted as blue dots, while the blue isosurfaces denote the changes in the bulk liquid over time, which is transported in *CRAFT CFD*® using an Eulerian frame.

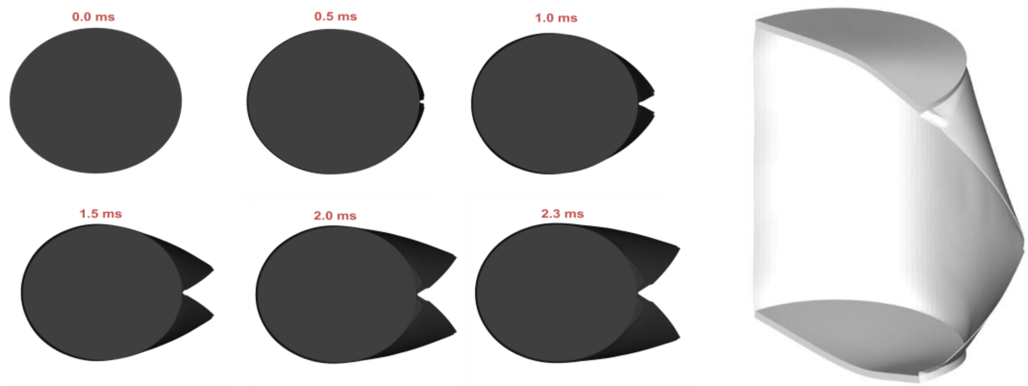

(a) Deformation at selected instants (b) Final deformed shape

Figure 7. Evolution of canister deformation.

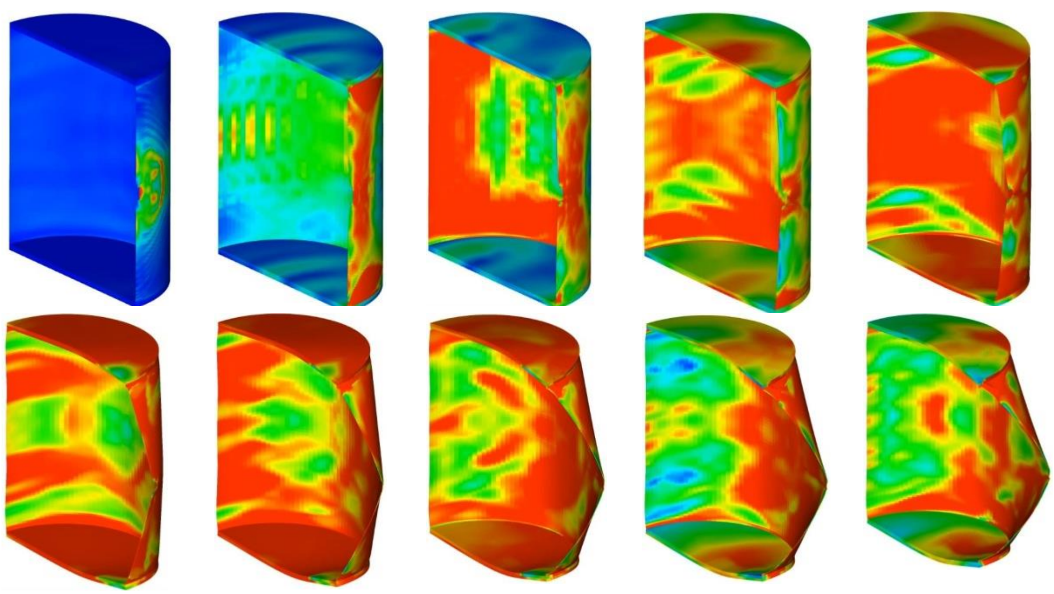

Figure 8. Evolution of stresses during canister rupture event.

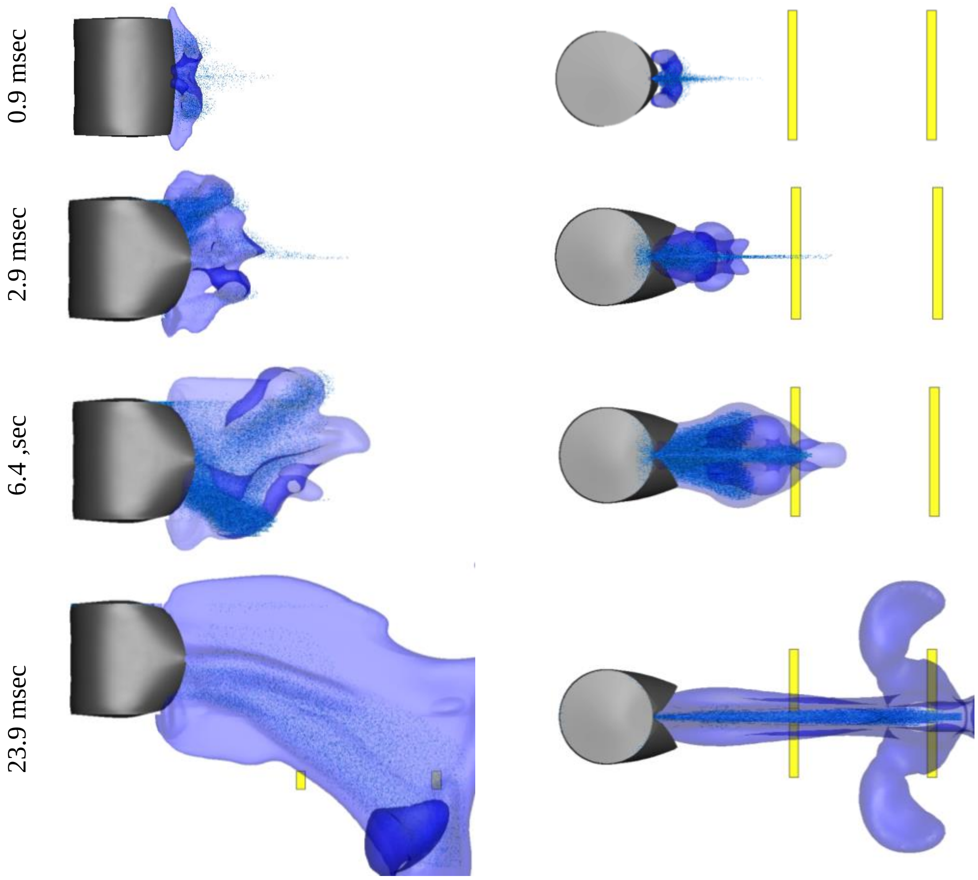

(a) Side view (b) Top View

Figure 9. Evolution of bulk water ejection from ruptured canister.

3.3 Plate Optimization

A new class of engine designs is under development for applications whose exhaust systems may include features such as compact, sinuous ducts with complex 3D non-axisymmetric shapes, fixed exit areas, thrust vectoring *etc*. The development of these exhaust systems requires that attention be directed towards the structural analysis in addition to the aerodynamic or flow path investigations. Structural concerns may be significant when the non-axisymmetric nozzle exhausts onto aircraft surfaces. In these situations, there is enhanced possibility of flow-induced vibrations for such structural surfaces that may suffer from prolonged and repeated exposure to high acoustic loading.

A sample design optimization of a simplified plate structure was exercised using the optimization framework depicted in Figure 10. The optimization algorithm is a multi-objective genetic algorithm, available as part of the DAKOTA package (Adams, 2009). DAKOTA performs the task of sampling the given design space and evaluating the function response to changes made in the design. Given new design parameters, the plate geometry is altered. The Sculptor code (Optimal) morphs or deforms the existing computational mesh to conform to the new shape dictated by the new design parameters. The updated mesh is preprocessed for analysis by Abaqus, which computes the structural response to the fluid loads. Post-processing of the Abaqus results is accomplished using Ensight (CEI), where the necessary functions to be evaluated are extracted. In the current demonstration, two competing objectives are sought. An optimal design is desired wherein peak stress is minimized and the weight is minimized.

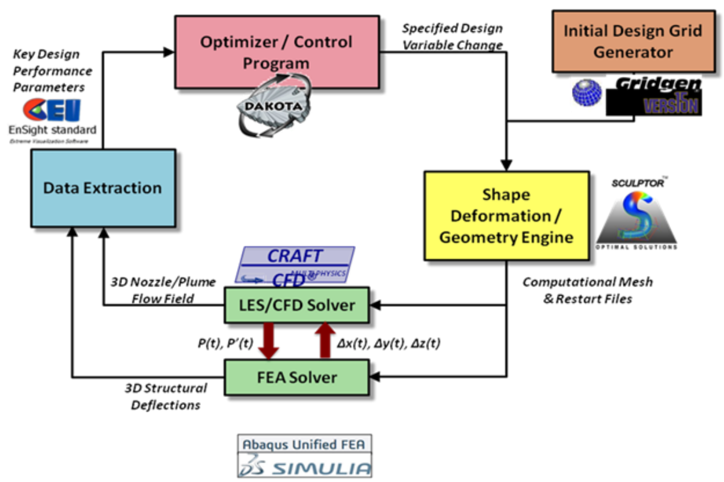

Figure 10. Design optimization process.

Analysis was performed for a generic nozzle plate configuration with twin, rectangular, high aspect ratio (AR=4) nozzles at an under-expanded nozzle pressure ratio (NPR) of 4.0. Transient one-way coupled structural analyses were conducted using Abaqus, given transient pressure histories provided by LES calculations using *CRAFT CFD*®. In each case the plate deflections observed were consistent with the first two dominant modes, and the plate response was largely vibrational in nature, with peak displacements on the order of the boundary layer thickness and peak velocities less than 0.1% of the jet velocity. As such the feedback to the jet is small and a one-way coupled approach is valid.

The baseline plate, which is intended to represent a deck surface over which the simulated rectangular jet exhausts, is 14" long in the streamwise direction and 16.5625" wide in the spanwise direction, with an assumed thickness of 0.1". The plate is constrained along the span

http://www.3ds.com/events/science-in-the-age-of-experience

parallel to the jet flow. Properties for AMS 5524 stainless steel are employed. For this initial demonstration, two design variables were altered. A deformation volume was created in Sculptor permitting the overall thickness of the plate and the thickness of two pre-defined reinforcing "ribs" to be varied. The reinforcing ribs were placed across the span of the plate. In the course of sampling the design space, many shapes were created, analyzed with Abaqus, and subsequently assessed. The design variations reflected varying plate thickness and rib thickness.

The optimization process results in a "Pareto front", shown in Figure 11. The Pareto front, represented by the set of blue points, represents satisfactory designs in which one of the objective functions is minimized. Therefore a design that minimizes stress is an acceptable design even though it may be heavy. Over the course of 11 generations of the genetic algorithm, 100 different designs were produced and analyzed. Some of these, indicated by the red points, are discarded, as the function objectives of weight and peak stress are behind the Pareto front of optimal solutions. It should be noted that as additional generations are evaluated, more designs would populate the Pareto front and fill in the gaps seen in Figure 11.

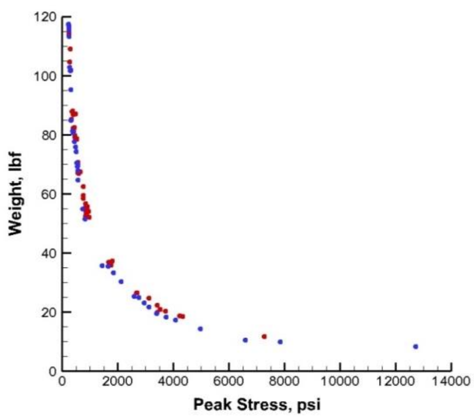

Figure 11. Designs produced, with Pareto front.

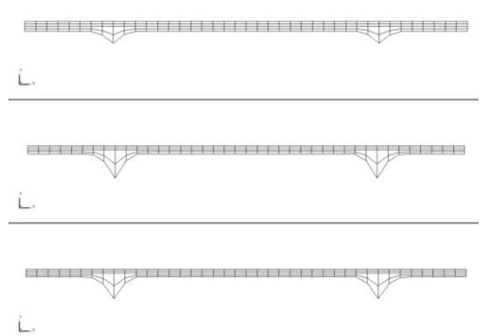

Figure 12. Candidate optimal designs.

Note that for the competing objectives of minimal weight and minimal peak stress, the optimal designs would be those near the 2000 psi mark on the Pareto front. Figure 12 presents three of these candidate designs. The tradeoff between plate thickness and rib thickness can be seen in each of these geometries. Figure 13 and Figure 14 show the resulting deformations and stresses produced with the optimum design. The ribs are thicker and the bending mode is largely broken up by this additional stiffness. Peak deformations are reduced with this design, at approximately 0.003 inches. In the best designs, peak stress was reduced, with the plate thickness increased relative to the baseline configuration.

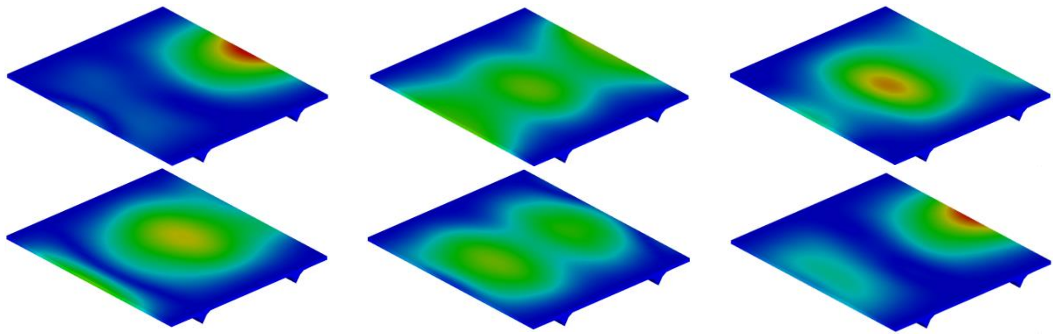

Figure 13. Deformations in candidate design 72 at selected intervals.

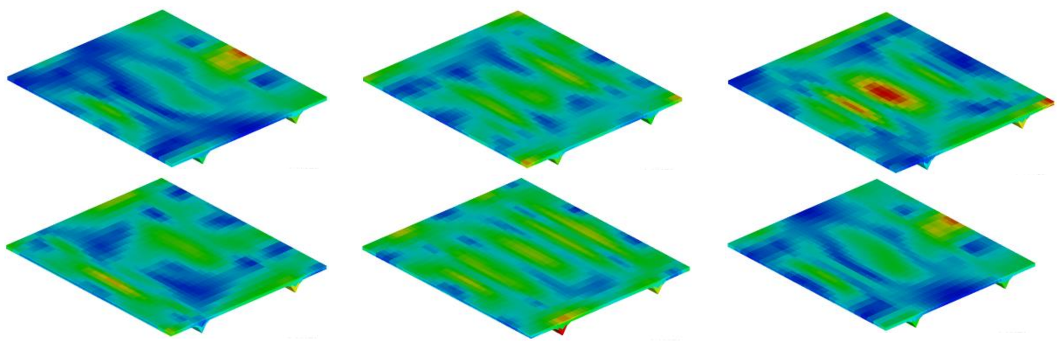

Figure 14. Stresses in candidate design 72 at selected intervals.

4. Concluding Remarks and Future Direction

Using the Co-Simulation Engine (CSE), structural dynamics predictions have been coupled with fluid flow analysis for challenging problems with complex physical modeling. One-way and two-way coupled CFD/FEA simulations have been successfully demonstrated for problems in aeroacoustics and vibration, conjugate heat transfer, bulk liquid release, and structural optimization. The use of Abaqus has favorably impacted our workflow and these early successes have led to increased interest and activity in the area of multidisciplinary applications for CRAFT Tech's aerospace and defense clients.

We at CRAFT Tech are continuing to increase our knowledge base and experience in using Abaqus for practical FSI applications. Potential application areas that are of interest for future studies include cyclic fatigue, anisotropic and sandwiched materials, damage evolution and failure, and problems involving concrete.

5. References

1. Adams, B.M., et al., "DAKOTA, A Multilevel Parallel Object-Oriented Framework for Design Optimization, Parameter Estimation, Uncertainty Quantification, and Sensitivity Analysis," Sandia National Laboratory Report SAND2010-2184, December 2009.
2. Allen, C.B., "Parallel Flow-Solver and Mesh Motion Scheme for Forward Flight Rotor Simulation," AIAA Paper 2006-3476, 24th Applied Aerodynamics Conference, San Francisco, CA, June 5-8, 2006.
3. Cavallo, P.A., Sinha, N., and Feldman, G.M., "Parallel Mesh Adaptation Method for Moving Body Applications," *AIAA Journal*, Vol. 43, No. 9, pp. 1937-1945.
4. CEI, Inc., https://www.ceisoftware.com/
5. Hosangadi, A., Lee, R.A., Cavallo, P.A., Sinha, N., and York, B.J., "Hybrid, Viscous, Unstructured Mesh Solver for Propulsive Applications," AIAA Paper 98-3153, 34th Joint Propulsion Conference, Cleveland, OH, July 13-15, 1998.
6. Kannepalli, C., Chartrand, C., Birkbeck, R., Sinha, N., and Murray, N., "Computational Modeling of Geometrically Complex Weapons Bays," AIAA Paper 2011-2774, 17th Aeroacoustics Conference.
7. Optimal Solutions, LLC, http://gosculptor.com/
8. Panickar, M., Murray, N., Jensen, B., Joachim, M., Birkbeck, R., Kannepalli, C., and Sinha, N., "Reduction of Noise Generated by Half-Open Weapons Bay," *Journal of Aircraft*, Vol. 50, No. 3, 2013.
9. Panickar, M.B., Murray, N.E., and Jansen, B.J., "Interactions Between Weapons Bay Cavity and Door in Mach 0.75 and 1.5 Flow," AIAA SciTech, January 2016.
10. Pointwise, Inc., http://www.pointwise.com
11. Simulia Abaqus suite, http://www.3ds.com/products/simulia/portfolio/ABAQUS/overview

6. Acknowledgments

This work was supported by funding from AFRL, DTRA, and NAVAIR. All computations were performed on DoD DSRC computing platforms. The author thanks Dr. Albert Kurkchubasche of SIMULIA for his invaluable assistance with integrating the Co-Simulation Engine.